Supporting Information

Olivier et al. 10.1073/pnas.1414401111

SI Materials and Methods

Chemical Synthesis of Negamycin. Negamycin was synthesized by a novel pathway using the previously described **1** (1) and invoking addition of methylacetate ion to the Ellman sulfinyl imine **2** to set the second stereocenter in 5:1 diastereoselectivity (2) (Fig. S1). Subsequent conversion to the hydrazide **5** followed by deprotection afforded synthetic negamycin, identical by NMR and liquid chromatography/mass spectrometry (LC/MS) to authentic fermentation negamycin, kindly provided by Dr. Yoshikazu Takahashi of the Microbial Research Institute, Tokyo, Japan. Negamycin exists as a 4:1 ratio of carboxamide geometrical isomers in D_2O as determined by NMR.

Synthesis of (*R*,*E*)-*N*-((*R*)-4-Azido-3-((*tert*-Butyldimethylsilyl)oxy) butylidene)-2-Methylpropane-2-Sulfinamide (2). (*R*)-4-Azido-3-((*tert*-butyldimethylsilyl)oxy)butanal (**1**) (1) (8.5 g, 34.93 mmol) was added to (*R*)-2-methylpropane-2-sulfinamide (4.66 g, 38.42 mmol), $CuSO_4$ (40 g) in CH_2Cl_2 (300 mL) at 25 °C. The resulting mixture was stirred at 25 °C for 24 h. The reaction mixture was filtered through silica gel, and the solvent of the filtrate was removed. The crude product was purified by flash silica gel chromatography, elution gradient 10–100% (vol/vol) petroleum ether in ethyl acetate (EtOAc). Pure fractions were evaporated to dryness to afford the title compound [7.0 g, 58% (mol/mol)] as a yellow oil. ^{1}H NMR (400 MHz, $CDCl_3$) δ 8.0 (t, 1H), 4.1 (m, 1H), 3.2 (dd, 1H), 3.14 (dd, 1H), 2.65–2.7 (m, 2H), 1.1 (s, 9H), 0.8 (s, 9H), 0.03 (s, 6H).

Synthesis of (3*S*,5*R*)-Methyl 6-Azido-5-((*tert*-Butyldimethylsilyl)oxy)-3-(1,1-Dimethylethylsulfinamido)hexanoate (3a). A solution of 2 M lithium diisopropylamide (LDA) (in THF) (8.66 mL, 17.3 mmol) was added dropwise over a period of 5 min under N_2 to a stirred mixture of **2** (3 g, 8.66 mmol) in 50 mL THF cooled to −78 °C. The resulting solution was stirred at −78 °C for 30 min. $TiCl_4$ (6.77 g, 26.0 mmol) in 2 mL THF was added at −78 °C, and the mixture was stirred for 2 h at that temperature. The reaction mixture was diluted with EtOAc, washed with H_2O and saturated aqueous (sat. aq.) solution of NaCl. The organic layer was dried Na_2SO_4, filtered and concentrated. The residue was purified by silica gel chromatography (1:1 petroleum ether/EtOAc) to afford the title compound [1.5 g, 41% (mol/mol)] as a yellow oil and (3*R*,5*R*)-methyl 6-azido-5-((tert-butyldimethylsilyl)oxy)-3-(1,1-dimethylethylsulfinamido)hexanoate (0.3 g) as a yellow oil. **3a**: ^{1}H NMR (400 MHz, $CDCl_3$) δ 4.37 (d, 1H), 3.0–4.0 (m, 1H), 3.64 (s, 3H), 3.3 (dd, 1H), 3.15 (dd, 1H), 2.95 (dd, 1H), 2.6 (dd, 1H), 1.8–1.9 (m, 1H), 1.55–1.7 (m, 1H), 1.25 (s, 9H), 0.9 (s, 9H), 0.1 (s, 6H). **3b**: ^{1}H NMR (400 MHz, $CDCl_3$) δ 4.35 (d, 1H), 3.0–4.0 (m, 1H), 3.65 (s, 3H), 3.3 (dd, 1H), 3.15 (dd, 1H), 2.95 (dd, 1H), 2.6 (dd, 1H), 1.8–1.9 (m, 1H), 1.55–1.7 (m, 1H), 1.2 (s, 9H), 0.9 (s, 9H), 0.1 (2s, 6H).

Synthesis of (3*R*,5*R*)-6-Azido-5-((*tert*-Butyldimethylsilyl)oxy)-3-(1,1-Dimethylethylsulfinamido)hexanoic Acid (4). LiOH (0.68 g, 28.5 mmol) in H_2O (1.0 mL) was added to a solution of **3a** in 20 mL MeOH. The mixture was stirred at room temperature for 2 h before being diluted with 0.5 N HCl and extracted with EtOAc. The EtOAc was washed with H_2O and sat. aq. NaCl. The organic layer was dried (Na_2SO_4), filtered, and concentrated to afford the title compound [3.50 g, 91% (mol/mol)] as a yellow oil. ^{1}H NMR (400 MHz, DMSO-d_6) δ 12.1 (br. s, 1H) 5.1 (d, 1H), 5.0–5.1 (m, 1H), 3.3–3.6 (m, 2H), 3.15 (dd, 1H), 2.4–2.5 (m, 1H), 2.3 (dd, 1H), 1.8–1.95 (m, 1H), 1.6–1.75 (m, 1H), 1.1 (s, 9H), 0.9 (s, 9H), 0.1 (s, 6H).

Synthesis of *tert*-Butyl 2-(2-((3*R*,5*R*)-6-Azido-5-((*tert*-Butyldimethylsilyl) oxy)-3-(1,1-Dimethylethylsulfinamido)hexanoyl)-1-Methylhydrazinyl) acetate (5). Diisopropylethylamine (1.271 g, 9.84 mmol) was added to a solution of **4**, 2-(3H-[1,2,3]triazolo[4,5-b]pyridin-3-yl)-1,1,3,3-tetramethylisouronium hexafluorophosphate(V) (2.244 g, 5.90 mmol), and tert-butyl 2-(1-methylhydrazinyl)acetate (0.946 g, 5.90 mmol in 20 mL THF. The mixture was stirred at room temperature for 2 h before being diluted with EtOAc. The EtOAc was washed with H_2O, sat. aq. $NaHCO_3$, and sat. aq. NaCl. The organic layer was dried (Na_2SO_4), filtered, and concentrated. The residue was purified by silica gel chromatography (10:1 CH_2Cl_2/MeOH) to afford the title compound [1.8 g, 67% (mol/mol)] as a yellow oil. ^{1}H NMR (400 MHz, $CDCl_3$) δ 8.1 (s, 1H) 5.0 and 5.05 (2d, 1H), 4.9–5.0 (m, 1H), 3.2–3.7 (m, 5H), 2.58 and 3.0 (2 dd, 1H), 2.7 (2s, 3H), 1.95 and 2.2 (2 dd, 1H), 1.6–1.85 (m, 2H), 1.45 (s, 9H), 1.2 (2s, 9H), 0.9 (2s, 9H), 0.1 (2s, 6H); ∼2.3:1 ratio of isomers.

Synthesis of *tert*-Butyl 2-(2-((3*R*,5*R*)-6-Amino-5-((*tert*-Butyldimethylsilyl) oxy)-3-(1,1-Dimethylethylsulfinamido)hexanoyl)-1-Methylhydrazinyl) acetate. A mixture **5** (3 g, 5.47 mmol), 10% (wt/wt) Pd on carbon (0.582 g) in 40 mL MeOH was stirred at room temperature for 4 h under an H_2 atmosphere. The reaction mixture was filtered through diatomaceous earth, and the filtrate was concentrated to afford the title compound [2.80 g, 98% (mol/mol)] as a yellow oil. ^{1}H NMR (400 MHz, MeOH-d_4) δ 4.1–4.2 (m, 1H), 3.6 (s, 1H), 3.3 (s, 1H), 3.0–3.15 (m, 1H), 2.7 (2s, 3H), 2.6–2.65 (m, 1H), 1.6 (s, 9H), 1.25 (s, 9H), 0.95 (s, 9H), 0.2 (2s, 6H).

Synthesis of 2-(2-((3*R*,5*R*)-3,6-Diamino-5-Hydroxyhexanoyl)-1-Methylhydrazinyl)acetic Acid (Negamycin). 4N HCl in dioxane (33.0 mL, 131.98 mmol) was added in one portion to 2.3 g (4.4 mmol) of the preceding compound in 30 mL dioxane at 25 °C, and the resulting mixture was stirred for 2 h. Solvent was removed, and the residue was triturated with Et_2O. The insoluble solids were collected by filtration, rinsed with 100 mL Et_2O, and dried under vacuum. The solids were purified by Dowex 50WX8-100 resin, eluting with 3% (wt/vol) aq. NH_4OH. The pure fractions were evaporated to dryness to afford the title compound [0.7 g, 64% (mol/mol)] as a white solid. ^{1}H NMR (400 MHz, D_2O) δ 4.01–4.1 (m, 1H), 3.5–3.75 (m, 1H), 3.45 (s, 2H), 3.15 (dd, 1H), 2.9–3.0 (m, 1H), 2.7 (s, 3H), 2.65 (m, 2H), 1.6–1.75 and 1.75–1.9 (2m, 2H, 4:1 ratio).

Isolation and Characterization of Negamycin-Resistant Mutants. *E. coli* strains containing a single rrn operon under kanamycin selection were obtained from the *E. coli* Genetic Stock Center. Negamycin-resistant mutants of SQ110 and SQ171 pHK-*rrnC* were isolated using previously published protocols (3). Antimicrobial activity was determined according to conditions defined by the Clinical and Laboratory Standards Institute (4). Whole-genome sequencing of mutants of SQ110 was performed as described elsewhere (5). Plasmids were isolated from mutants of SQ171 pHK-*rrnC* and transformed into SQ171-pKK3535, as described previously (6). Plasmids that transferred both kanamycin and negamycin resistance were sequenced.

Coupled in Vitro Transcription–Translation Assays. Coupled in vitro transcription–translation assays using S30 extract from *E. coli* were performed according to Buurman et al. (7) with modifications in compound preparation. Specifically, compounds were dissolved and serially diluted in water instead of in DMSO. To compensate for the 1% DMSO in the reaction, 2% (vol/vol)

DMSO was added to reagent 1, containing S30 extract. When present, TetM proteins were added to twice the final concentration in reagent 2, containing nucleotides, amino acids, and plasmid. Coupled in vitro transcription–translation assays using purified, recombinant components from *E. coli* were performed using PURExpress In Vitro Protein Synthesis Kits lacking native ribosomes (New England Biolabs).

Tetracycline Competition Assays. Binding of compounds to empty ribosomes was conducted similar to the method described by Grossman et al. (8) using radiolabeled [3H] tetracycline (American Radiolabeled Chemicals). Briefly, 25-μL reactions in duplicate contained 4 μM 70S *E. coli* ribosomes purified from the strain MRE 600 (Paragon) in binding buffer (20 mM Tris-acetate at pH 7.5, 15 mM $MgCl_2$, 150 mM NH_4Cl, 2.5 mM DTT, 2.5 mM TCEP, 1 mM putrescine, 5 mM spermidine). To each reaction, radiolabeled tetracycline stock was added to a final concentration of 20 μM with a specific activity of 226 counts/pmol, which equated to 50% binding from the saturation curve. To measure the IC_{50} for each compound, reactions were performed in the absence or presence of increasing concentrations of the competing compound and incubated at 37 °C for 15 min. From each reaction, 5 μL was removed and diluted with 80 μL of ice-cold binding buffer and passed through a UniFilter GF/B Barex filter plate using a FilterMate Universal Harvester (PerkinElmer). Filters were washed with a quick pulse of water and subsequently dried at 37 °C for 1 h. A volume of 50 μL of MicroScint-20 scintillation fluid (PerkinElmer) was added to each well and the plate analyzed for radioactivity using a TopCount liquid scintillation counter (PerkinElmer).

Aminoacylation and Fluorescent Labeling of tRNA for Single-Molecule Fluorescence. $tRNA^{fMet}$ and $tRNA^{Phe}$ from *E. coli* strain MRE 600 were purified as previously described (9). Aminoacylation, formylation, and fluorescent labeling of tRNA were performed as previously described (10). With this approach, Cy3 and photostabilized Cy5 dyes (11) were site-specifically attached through either maleimide or *N*-hydroxysuccinimide chemistry to $tRNA^{fMet}(s^4U8)$ and $tRNA^{Phe}(acp^3U47)$ at naturally occurring modified base residues located near the elbow region of the tRNA body. Cy5 was photostabilized as previously described (11), with two additional sulfonate groups added for enhanced solubility. Charging of $tRNA^{Phe}$ was achieved using recombinant phenylalanyl tRNA synthetase (PheRS) prepared as previously described (10, 12, 13). Dye-labeled tRNAs prepared in this manner are fully competent in tRNA selection, translocation, and peptide bond formation (10).

Preparation of Ribosome Complexes for Single-Molecule Imaging. Initiation complexes were prepared from 30S and 50S ribosomal subunits (1 μM each) isolated from *E. coli* as described for crystallographic investigations. Complexes were initiated in vitro on cognate (UUC) or near-cognate (UCU) mRNAs derived from the gp32 gene product bearing a 5′-biotin moiety (5′-biotin-CAA CCU AAA ACU UAC ACA CCC UUA GAG GGA CAA UCG AUG **U(UC/CU)** AAA GUC UUC AAA GUC AUC) (Dharmacon) in the presence of IF-1 (2 μM), IF-2 (2 μM), IF-3 (2 μM), 2 mM GTP, and fMet-$tRNA^{fMet}$(Cy3-s^4U8) in Tris-polymix buffer containing 50 mM Tris-acetate, pH 7.5; 5 mM Mg$(OAc)_2$; 100 mM KCl; 5 mM NH_4OAc; 0.5 mM $CaCl_2$; 0.1 mM EDTA; 5 mM putrescine; and 1 mM spermidine, as previously described (10).

Single-Molecule Fluorescence Experiments and Data Processing. All experiments were performed in Tris-polymix buffer containing 50 mM Tris-acetate, pH 7.5; 5 mM Mg$(OAc)_2$; 100 mM KCl; 5 mM NH_4OAc; 0.5 mM $CaCl_2$; 0.1 mM EDTA; 5 mM putrescine; 1 mM spermidine; 1.5 mM β-mercaptoethanol; and 100 μM GTP, in the presence of an oxygen scavenging environment [2 mM protocatechuic acid, 50 nM protocatechuate 3,4-dioxygenase containing a mixture of triplet-state quenching compounds (1 mM Trolox, 1 mM cyclooctatetraene, 1 mM nitrobenzyl alcohol) (14)]. The ternary complex of EF-Tu•GTP•Phe-$tRNA^{Phe}$(Cy5-acp^3U47) was prepared following established procedures (15, 16). Ribosome complexes (0.5 nM) programmed with biotinylated mRNA were surface immobilized following brief incubation within PEG-passivated, streptavidin-coated quartz microfluidic devices (13). To avoid contributions of hybrid states formation following accommodation, the amino acid on P site tRNA was released by incubating immobilized ribosomes with 2 mM puromycin (Sigma) for 10 min before ternary complex delivery.

smFRET data were acquired by using a prism-based total internal reflection microscope as previously described (13). The Cy3 fluorophore linked to $tRNA^{fMet}$ was excited by the evanescent wave generated by total internal reflection of a single frequency light source (Opus 532 nm, Laser Quantum). Photons emitted from both Cy3 and Cy5 were collected by using a 1.27 N.A. 60× water-immersion objective (Nikon), in which optical treatments were used to spatially separate Cy3 and Cy5 frequencies onto two cooled, back-thinned EMCCD cameras (Evolve 512; Photometrics). Fluorescence data were acquired using MetaMorph acquisition software (Universal Imaging Corporation) with an integration time of 15 ms. FRET trajectories were calculated from fluorescence traces by using the formula $FRET = I_{Cy5}/(I_{Cy3} + I_{Cy5})$, where I_{Cy3} and I_{Cy5} represent the Cy3 and Cy5 fluorescence intensities, respectively. Fluorescence and FRET traces were selected for analysis by using semiautomated smFRET automated analysis software implemented in MATLAB (MathWorks) as previously described (17).

Crystallography. X-ray diffraction data were collected at the IMCA-CAT beamline 17-ID with the Pilatus 6M detector from vitrified crystals under cryogenic conditions using 0.1° oscillations and exposure times of 0.15 s per frame with the beam attenuated by 40%. All diffraction data were collected from a single crystal. Use of the IMCA-CAT beamline 17-ID at the Advanced Photon Source was supported by the companies of the Industrial Macromolecular Crystallography Association through a contract with Hauptman-Woodward Medical Research Institute. Use of the Advanced Photon Source was supported by the US Department of Energy, Office of Science, Office of Basic Energy Sciences, under Contract DE-AC02-06CH11357. Diffraction data were indexed with XDS (18) and scaled using Aimless (19), as defined in the autoPROC routines within the Global Phasing software suite (20). The crystal structure of two 70S particles in the asymmetric unit was determined by molecular replacement using Phaser (21) and coordinates of the *E. coli* 70S ribosome in the apo state (PDB ID codes 3i1m, 3i1n, 3i1o, 3i1p) (22). Rigid-body refinement initially was conducted at low resolution by using the 30S and 50S particles as the rigid domains using the lmr program. Crystallographic refinement was carried out using autoBUSTER (23) or PHENIX (24). Noncrystallographic symmetry and target restraints were used (25), and translation/libration/screw rotation refinement was used in the refinement. Coot (26) was used to analyze the electron density maps, manual model rebuilding, and inhibitor placement. The refinement dictionary for negamycin was generated with GRADE (27) and the stereochemistry checked with MOGUL (28).

Recombinant TetM Preparation. The *tetM* gene from *Enterococcus faecalis* was codon-optimized for expression in *E. coli* and custom-synthetized as 6His-TEV-TetM (2-639) (Blue Sky BioServices). The optimized gene was cloned into pET-24a(+) (Novagen Biosciences) using NdeI and XhoI restriction sites to create plasmid pNG054. For protein overproduction, the plasmid was transformed into BL21(DE3) (EMD Chemicals) and plated on Luria–Bertani (LB) plates containing 25 μg/mL kanamycin, and incubated at 37 °C

overnight. A single colony of BL21(DE3)/pNG054 was inoculated into a 100-mL culture of LB containing 25 μg/mL kanamycin and grown overnight at 37 °C. The overnight culture was diluted to OD_{600} = 0.1 in 4 × 1 L of LB containing 25 μg/mL kanamycin and grown at 37 °C with aeration to midlogarithmic phase (OD_{600} = 0.6). The culture was incubated on ice for 30 min and transferred to 18 °C. Isopropyl β-D-1-thiogalactopyranoside then was added to a final concentration in each culture of 0.5 mM. After overnight induction at 18 °C, the cells were harvested by centrifugation at 5,000 × *g* for 15 min at 25 °C. Cell pastes were stored at –20 °C. The frozen cell pastes from 4 L cell culture were suspended in 50 mL of lysis buffer consisting of 25 mM Tris·HCl (pH 8.0), 0.5 M NaCl, 5% (vol/vol) glycerol, and one protease inhibitor mixture tablet EDTA-free (Roche Molecular Biochemical). Cells were disrupted twice by using French press at 18,000 psi at 4 °C, and the crude extract was centrifuged at 150,000 × *g* (45Ti rotor; Beckman-Coulter) for 30 min at 4 °C. The supernatant was applied at a flow rate of 2.0 mL/min onto a 5-mL HiTrap Ni^{2+} chelating column (GE Healthcare Life Sciences) pre-equilibrated with Buffer A containing 25 mM Tris·HCl (pH 8.0), 0.5 M NaCl, 5% (vol/vol) glycerol. The column then was washed with Buffer A, and the TetM was eluted by a linear gradient from 0 M to 0.5 M imidazole in Buffer A. Fractions containing TetM were pooled, and dialyzed against 2 L of Buffer B [25 mM Hepes, pH 7.3; 1 mM EDTA; 1 mM DTT; 5% glycerol (vol/vol)] overnight at 4 °C. The dialyzed sample was applied at a flow rate of 2.0 mL/min onto a 20-mL Q Sepharose HP (HR16/10) column (GE Healthcare Life Sciences) pre-equilibrated with Buffer B. After the column was washed with 100 mL of Buffer B, the protein was eluted by a linear gradient from 0 M to 1 M NaCl in Buffer B. The fractions containing TetM were pooled and concentrated by Amicon Ultracel-10K (Millipore). The protein concentration was determined by the Bradford method (29) and characterized by SDS/PAGE analysis and analytical LC-MS [expected molecular weight (MW) = 74,166 Da; observed MW = 74,165 Da]. The protein was stored at –80 °C.

1. Nishiguchi S, et al. (2010) Total synthesis of (+)-negamycin and its 5-epi-derivative. *Tetrahedron* 66(1):314–320.
2. Tang TP, Ellman JA (2002) Asymmetric synthesis of beta-amino acid derivatives incorporating a broad range of substitution patterns by enolate additions to tert-butanesulfinyl imines. *J Org Chem* 67(22):7819–7832.
3. Buurman ET, Johnson KD, Kelly RK, MacCormack K (2006) Different modes of action of naphthyridones in gram-positive and gram-negative bacteria. *Antimicrob Agents Chemother* 50(1):385–387.
4. Clinical and Laboratory Standards Institute (2009) *M07-A8: Methods for Dilution Antimicrobial Susceptibility Tests for Bacteria That Grow Aerobically; Approved Standard* (Clinical and Laboratory Standards Institute, Wayne, PA), 9th Ed, Vol 29-2.
5. Alm RA, et al. (2014) Analysis of *Staphylococcus aureus* clinical isolates with reduced susceptibility to ceftaroline: an epidemiological and structural perspective. *J Antimicrob Chemother*, 10.1093/jac/dku114.
6. Asai T, Zaporojets D, Squires C, Squires CL (1999) An *Escherichia coli* strain with all chromosomal rRNA operons inactivated: Complete exchange of rRNA genes between bacteria. *Proc Natl Acad Sci USA* 96(5):1971–1976.
7. Buurman ET, et al. (2012) Novel rapidly diversifiable antimicrobial RNA polymerase switch region inhibitors with confirmed mode of action in *Haemophilus influenzae*. *J Bacteriol* 194(20):5504–5512.
8. Grossman TH, et al. (2012) Target- and resistance-based mechanistic studies with TP-434, a novel fluorocycline antibiotic. *Antimicrob Agents Chemother* 56(5):2559–2564.
9. Dunkle JA, et al. (2011) Structures of the bacterial ribosome in classical and hybrid states of tRNA binding. *Science* 332(6032):981–984.
10. Blanchard SC, Gonzalez RL, Kim HD, Chu S, Puglisi JD (2004) tRNA selection and kinetic proofreading in translation. *Nat Struct Mol Biol* 11(10):1008–1014.
11. Zheng Q, et al. (2012) On the mechanisms of cyanine fluorophore photostabilization. *J Phys Chem Lett* 3(16):2200–2203.
12. Blanchard SC, Kim HD, Gonzalez RL, Jr, Puglisi JD, Chu S (2004) tRNA dynamics on the ribosome during translation. *Proc Natl Acad Sci USA* 101(35):12893–12898.
13. Munro JB, Altman RB, O'Connor N, Blanchard SC (2007) Identification of two distinct hybrid state intermediates on the ribosome. *Mol Cell* 25(4):505–517.
14. Dave R, Terry DS, Munro JB, Blanchard SC (2009) Mitigating unwanted photophysical processes for improved single-molecule fluorescence imaging. *Biophys J* 96(6):2371–2381.
15. Burnett BJ, et al. (2013) Elongation factor Ts directly facilitates the formation and disassembly of the Escherichia coli elongation factor Tu·GTP·aminoacyl-tRNA ternary complex. *J Biol Chem* 288(19):13917–13928.
16. Burnett BJ, et al. (2014) Direct evidence of an elongation factor-Tu/Ts·GTP·aminoacyl-tRNA quaternary complex. *J Biol Chem* 289(34):23917–23927.
17. Geggier P, et al. (2010) Conformational sampling of aminoacyl-tRNA during selection on the bacterial ribosome. *J Mol Biol* 399(4):576–595.
18. Kabsch W (2010) XDS. *Acta Crystallogr D Biol Crystallogr* 66(Pt 2):125–132.
19. Evans PR, Murshudov GN (2013) How good are my data and what is the resolution? *Acta Crystallogr D Biol Crystallogr* 69(Pt 7):1204–1214.
20. Vonrhein C, et al. (2011) Data processing and analysis with the autoPROC toolbox. *Acta Crystallogr D Biol Crystallogr* 67(Pt 4):293–302.
21. McCoy AJ, et al. (2007) Phaser crystallographic software. *J Appl Cryst* 40(Pt 4):658–674.
22. Zhang W, Dunkle JA, Cate JH (2009) Structures of the ribosome in intermediate states of ratcheting. *Science* 325(5943):1014–1017.
23. Bricogne G, et al. (2011) *Buster V2.11.5* (Global Phasing Ltd., Cambridge, UK).
24. Adams PD, et al. (2010) PHENIX: A comprehensive Python-based system for macromolecular structure solution. *Acta Crystallogr D Biol Crystallogr* 66(Pt 2):213–221.
25. Smart OS, et al. (2012) Exploiting structure similarity in refinement: Automated NCS and target-structure restraints in BUSTER. *Acta Crystallogr D Biol Crystallogr* 68(Pt 4):368–380.
26. Emsley P, Lohkamp B, Scott WG, Cowtan K (2010) Features and development of Coot. *Acta Crystallogr D Biol Crystallogr* 66(Pt 4):486–501.
27. Smart OS, et al. (2011) *GRADE, V1.101* (Global Phasing, Ltd., Cambridge, UK).
28. Bruno IJ, et al. (2004) Retrieval of crystallographically-derived molecular geometry information. *J Chem Inf Comput Sci* 44(6):2133–2144.
29. Bradford MM (1976) A rapid and sensitive method for the quantitation of microgram quantities of protein utilizing the principle of protein-dye binding. *Anal Biochem* 72:248–254.

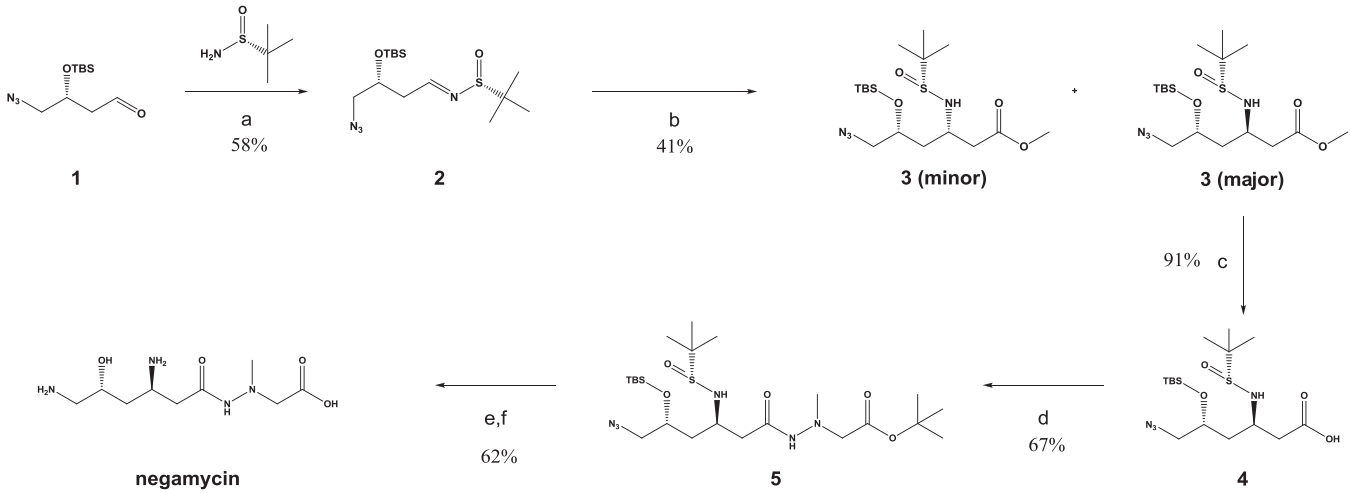

Fig. S1. Negamycin was synthesized by a novel pathway using the previously described **1** and invoking addition of methylacetate ion to the Ellman sulfinyl imine **2** to set the second stereocenter in 5:1 diastereoselectivity. Subsequent conversion to the hydrazide **5** followed by deprotection afforded synthetic negamycin. Reagents and conditions: (a) $CuSO_4$, CH_2Cl_2; (b) AcOMe, LDA, $ClTi(O\text{-}i\text{-}Pr)_3$; (c) LiOH, THF; (d) H_2, Pd/C; (e) HCl, dioxane; (f) ion-exchange purification.

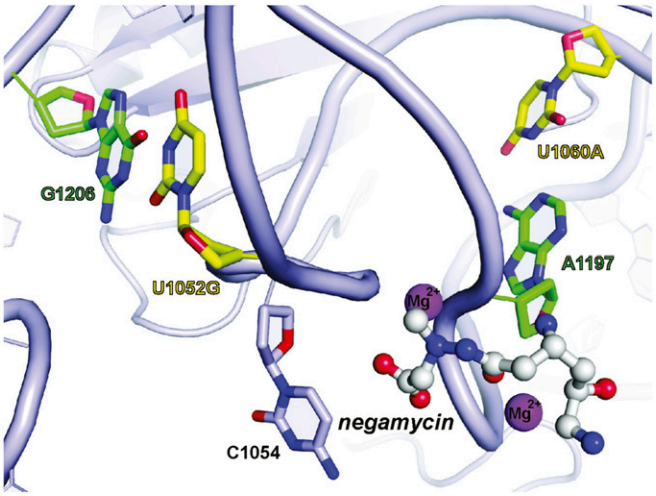

Fig. S2. Negamycin resistance mutations map to the small subunit head domain close to the h34 region of the *E. coli* ribosome. Nucleotides that conferred resistance when mutated are in yellow, corresponding base pairs in the native state are in green. Negamycin, C1054, and magnesium ions in close proximity are shown for reference.

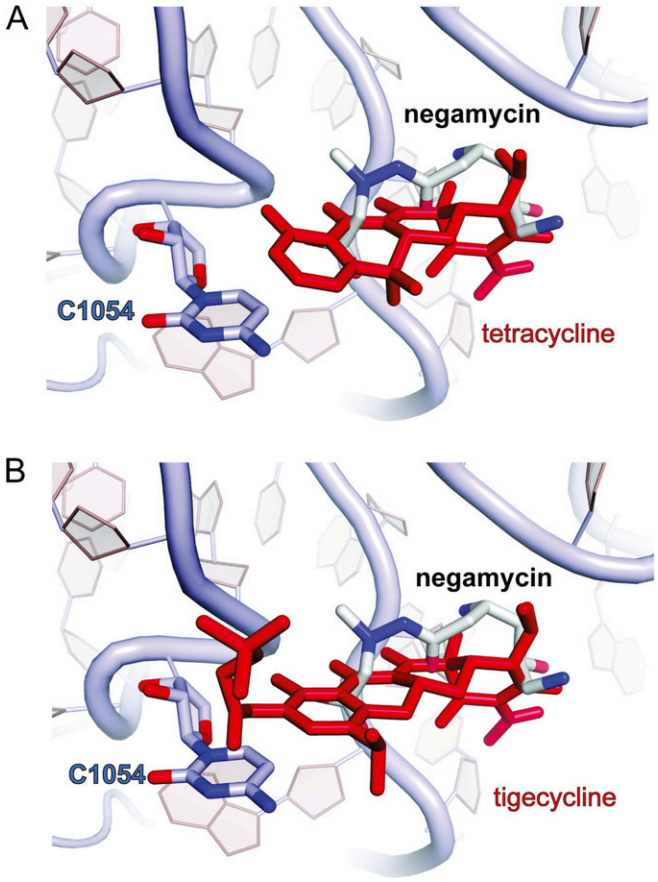

Fig. S3. Superposition of the 70S ribosome–negamycin complex on (*A*) the 70S ribosome–tetracycline complex (PDB ID code 4g5k) and (*B*) the 70S ribosome–tigecycline complex (PDB ID code 4g5t) based on residues 935–1,377 of the small subunit head domain (average rmsd ~0.57 Å).

Table S1. IC_{50} values for TetM vs. tetracycline, tigecycline, and negamycin in coupled in vitro transcription–translation assays using S30 extracts from *E. coli*

	Tetracycline		Tigecycline		Negamycin	
TetM, μM	IC_{50}, μM	Hill slope	IC_{50}, μM	Hill slope	IC_{50}, μM	Hill slope
0	1.46	1.04	0.30	1.18	1.74	1.40
0.01	20	0.96	0.39	1.38	1.92	1.54
0.1	42	0.67	0.46	1.45	1.91	1.66

Table S2. X-ray data collection and refinement statistics

Data processing	
Beamline	17-ID
Wavelength, Å	1.0000
Space group	$P2_12_12_1$
Unit cell dimensions	a = 211.91 Å, b = 434.30 Å, c = 624.39 Å; $\alpha = \beta = \gamma = 90°$
Resolution, Å	41.14–3.09 (3.096–3.086)
R_{merge}*	0.026 (0.129)
Total number of reflections	6,209,734 (58,709)
Total number of unique reflections	1,043,787 (10,419)
$\langle I/\sigma I \rangle$	14.9 (2.1)
Completeness, %	100 (99.8)
Multiplicity	5.9 (6.1)
CC(1/2)[†]	0.995 (0.640)
Refinement	
Resolution, Å	41.39–3.09
R_{work}[‡]/R_{free}[§], %	20.18/24.44

*$R_{merge} = \Sigma|I - \langle I \rangle|/\Sigma I$, where I is the integrated intensity of a given reflection and $\langle I \rangle$ is the average intensity of multiple observations of symmetry-related reflections.

[†]Ref. 1.

[‡]$R_{work} = \Sigma||F_o| - |F_c||/\Sigma|F_o|$, where F_o and F_c are observed and calculated structure factors.

[§]R_{free} was calculated from a 5% subset of reflections that were excluded from the refinement. Brackets indicate the highest-resolution shell.

1. Karplus PA, Diederichs K (2012) Linking crystallographic model and data quality. *Science* 336(6084):1030–1033.

Table S3. Tabulation of selected compounds exemplified in the literature with activity data generated from coupled in vitro transcription–translation assays using S30 extracts from *E. coli*

Structure	Name	Ref. (comp. no.)	$TT_{E.co,}$ μM
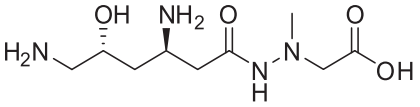	Negamycin	1 (1)	1.0
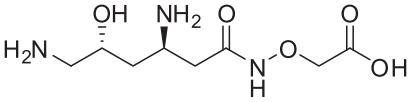	Hydroxamate	1 (36)	>80
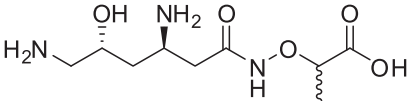	Methyl hydroxamate	1 (34)	>80
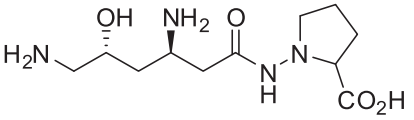	RHS constrained	1 (39)	>80
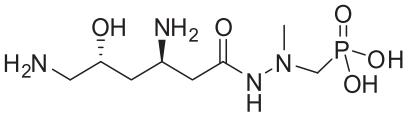	Phosphonic acid	1 (45)	>80
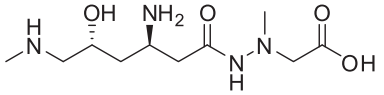	N6-methyl	1 (19a)	2.3
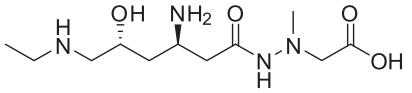	N6-ethyl	1 (19b)	4.5
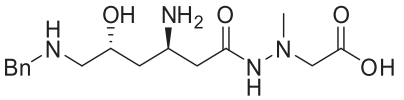	N6-benzyl	1 (16a)	0.8
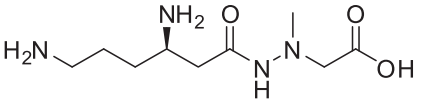	Deoxynegamycin	2 (1b)	8.2
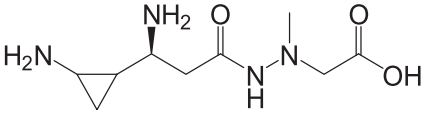	Cyclopropylamine	2 (35e2)	1.0

comp., compound; RHS, right-hand side.

1. Raju B, et al. (2003) N- and C-terminal modifications of negamycin. *Bioorg Med Chem Lett* 13(14):2413–2418.
2. Raju B, et al. (2004) Conformationally restricted analogs of deoxynegamycin. *Bioorg Med Chem Lett* 14(12):3103–3107.